Toward sub-Kelvin resistive cooling and non destructive detection of trapped non-neutral

electron plasma

Toward sub-Kelvin resistive cooling and non destructive detection of trapped non-neutral electron plasma

S. Di Domizio,[a,b] **D. Krasnický,**[a] **V. Lagomarsino,**[a] **G. Testera,**[a,1] **R. Vaccarone**[a] **and S. Zavatarelli**[a]

[a]*Istituto Nazionale di Fisica Nucleare,*
Via Dodecaneso 33, 16146 Genova, Italy

[b]*Università di Genova, Dipartimento di Fisica,*
Via Dodecaneso 33, 16146 Genova Italy

E-mail: testera@ge.infn.it

ABSTRACT: A resonant circuit tuned to a particular frequency of the motion of charged particles stored in a Penning trap and connected to a low noise amplifier allows, at the same time, cooling and non destructive detection of the particles. Its use is widely diffused when single or few particles are stored near the centre of a hyperbolic Penning trap. We present a consistent model that predicts the shape of the induced signal when the tuned circuit is used to detect and cool the axial motion of a cold non neutral plasma stored in an open-ended cylindrical Penning trap. The model correctly accounts for the not negligible axial plasma size. We show that the power spectrum of the signal measured across the tuned circuit provides information about the particle number and insights about the plasma temperature. We report on the design of a HEMT-based cryogenic amplifier working at 14.4 MHz and 4.2 K and the results of the noise measurements. We have measured a drain current noise in the range from 6 to 17 pA/$\sqrt{\text{Hz}}$, which corresponds to an increase of the tuned circuit equivalent temperature of at maximum 0.35 K. The cryogenic amplifier has a very low power consumption from few tens to few hundreds of μW corresponding to a drain current in the range 100–800 μA. An additional contribution due to the gate noise has been identified when the drain current is below 300 μA; above that value an upper limit of the increase of the equivalent tuned circuit temperature due to this contribution of 0.02 K has been obtained. These features make the tuned circuit connected to this amplifier a promising device for detecting and cooling the axial motion of an electron plasma when the Penning trap is mounted inside a dilution refrigerator.

KEYWORDS: Low-energy ion storage; HEMT amplifiers; Charge induction

---

[1]Corresponding author.

Contents

1 Introduction

This paper discusses the use of a radio-frequency resonator (tuned circuit) coupled to a low noise cryogenic amplifier to cool and detect a non-neutral electron plasma trapped in a Penning trap.

The work was performed in the context of the AEḡIS experiment [1] actually installed at CERN who is aiming to cool a large number (10^5 or more) of trapped antiprotons to a sub-Kelvin temperature and produce a cold anti-hydrogen beam to test the validity of the equivalence principle for antimatter [2]. One of the routes toward the sub-Kelvin antiproton cooling is their sympathetic cooling through collisions with simultaneously trapped electrons, which in turn are resistively cooled. This technique requires the use of a radio-frequency resonator anchored to the lowest possible temperature, eventually inside a dilution refrigerator. The use of such tuned circuit is well established in case of single or few particles (electrons or ions) stored near the centre of a Penning trap [3, 4] and it is known to play a crucial role as a cooling circuit as well as a diagnostic tool. Not much information is available on the use of this technique with trapped non-neutral plasmas.

This paper addresses two items relevant for the use of the tuned circuit and the cryogenic amplifier in the context of cooling of an electron plasma to sub-Kelvin temperatures. The first (presented in section 2) is the response of the circuit when many particles are present in the Penning trap. This is of interest to AEgIS and also to many other experiments dealing with large number of trapped charged particles. In this case the particles form a non-neutral plasma [5], whose axial size is not negligible when compared to the trap length. For this reason the few particle description is no longer adequate. We developed a consistent model describing the signal induced on the tuned circuit by a non-neutral plasma trapped in the harmonic potential of a Penning trap when it has reached the equilibrium temperature of the circuit.

The second item is discussed in section 3 of this paper. It is the realisation of a low noise, high gain and low power consumption cryogenic amplifier based on a high electron mobility transistor (HEMT) operated in a frequency range typical for trapped electrons (specifically our circuit is tuned to 14.4 MHz) and at the temperature of 4.2 K. This device shows features appealing for its use also in a sub-Kelvin trap environment. In fact our cryogenic amplifier circuit presents an equivalent noise temperature of the order of 0.2-0.3 K (depending on the drain current) at 4.2 K and it exhibits a very low power consumption between 10–$400\,\mu$W. These features, particularly the second one, make the device a very promising tool to be used in a dilution refrigerator as planned in AEgIS.

2 Tuned circuit particle detection in Penning traps

2.1 Detection of low number of particles in a Penning trap

A particle confined in a Penning trap induces charges on the surrounding electrodes and its motion creates a time-varying current through a circuit connected to them. This induced current allows a non destructive detection and cooling of the particle as it was proposed in [3]. According to [6], the charge $Q_j(\vec{r})$ induced on a electrode j depends on the position of the particle $\vec{r}$ through

$$Q_j(\vec{r}) = qW_j(\vec{r}), \tag{2.1}$$

where $W_j(\vec{r})$ is a weighting field calculated as the ratio between the potential in the position of the particle and the potential applied to the electrode j, with all the other electrodes grounded. The current i_j is obtained taking the time derivative of the previous relation:

$$i_j = q\vec{v} \cdot \vec{\nabla} W_j(\vec{r}), \tag{2.2}$$

$\vec{v}$ is the particle velocity and q is its charge. When a single or few particles are trapped near the centre of a Penning trap the current induced by the axial motion (with velocity v_z) is well approximated by

$$i = q\frac{v_z \alpha_0}{2z_0}, \tag{2.3}$$

where z_0 is the length from the centre to the end-cap of the Penning trap and the geometrical factor $\alpha_0 < 1$ depends only on the trap geometry.

The detection circuit (see figure 1) is usually not a simple resistor, but a LC resonant ("tuned") circuit obtained by connecting an inductor L_t to an electrode. The capacitance C_t is usually dominated by the trap electrode capacitance and the cable connections. In this way the on-resonance impedance of the circuit is purely resistive. The signal created on the inductor is then fed to the input of a low-noise amplifier. The resonance frequency of the circuit $\omega_0 = \dfrac{1}{\sqrt{L_t C_t}}$ matches the axial frequency of the particle. Typical values are in the range of 8–20 MHz in case of electrons and trap parameters of our interest.

The radio-frequency losses of the tuned circuit are represented by a series resistance r_s. We thus have a series $r_s L_t C_t$ circuit with an input current induced by the trapped particles. The noise of this detection technique originates mainly from the amplifier chain and from the Johnson noise V_{nt} of the r_s whose mean spectral power is $\overline{v}_{nt}^2 = 4KT_0 r_s \Delta f$, where K is the Boltzmann constant, T_0 is the circuit temperature and Δf is the bandwidth.
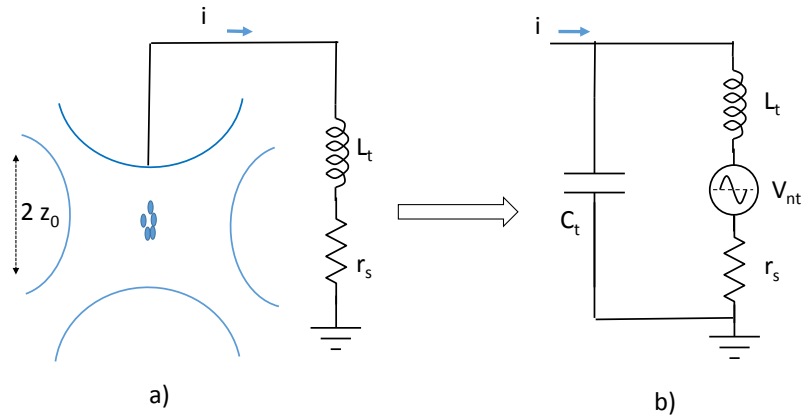
Figure 1. (a) Current induced by few particles trapped near the center of a hyperbolic Penning trap and tuned circuit connected to the end-cap. (b) Equivalent resonant circuit including the noise associated to the resistor.

The quality factor of the resonance Q is given by $Q = \omega_0 L_t / r_s$. In literature the detection circuit is often modelled as a parallel $R_d L_t C_t$ circuit with a quality factor $Q = R_d / \omega_0 L_t$ and a so-called parallel dynamic resistance $R_d = r_s Q^2$.

2.2 Resistive cooling of particles

As was mentioned earlier, the detection circuit of figure 1 can also serve to reduce the energy of trapped particles [4] since the voltage across the circuit generates an electric field, which acts on them. This voltage has two contributions: one due to the current induced by the particles and one due to the noise V_{nt}. The former is responsible for the cooling and the latter sets the ultimate limit on the achievable temperature. The energy of the particles exponentially decreases with a rate γ_{rc}

$$\gamma_{rc} = \frac{q^2 \alpha_0^2 R_d}{4 z_0^2 m} = \frac{q^2 \alpha_0^2 Q^2 r_s}{4 z_0^2 m} \tag{2.4}$$

and it reaches the equilibrium value $K(T_0 + T_{\mathrm{add}})$ where T_0 is the temperature of the tuned circuit and T_{add} is the equivalent temperature due to the noise of the amplifier. For this reason the detection system must be anchored to the lowest possible temperature of the apparatus and the equivalent noise temperature of the amplifier should be minimized.

It has been shown in [7] that the tuned circuit provides a non-destructive diagnostic of the particles confined near the trap's centre when they are in equilibrium with the detection circuit. The spectral power of the signal across the tuned circuit measured at equilibrium shows a resonance curve with a "dip" at the frequency of particle motion: from the form of this signal one can deduce the number of trapped particles [7, 12]. In addition monitoring the output spectral power density of the tuned circuit during the cooling process provides insights about the cooling rate.

2.3 Non-neutral plasmas and the AEgIS anti-hydrogen production trap

The AEḡIS trap system includes several cylindrically shaped electrodes mounted inside the bore of a superconducting magnet. Some of them are located in a 5 T magnetic field and in a 10 K environment while other electrodes are mounted in a region with a lower field of 1 Tesla and inside
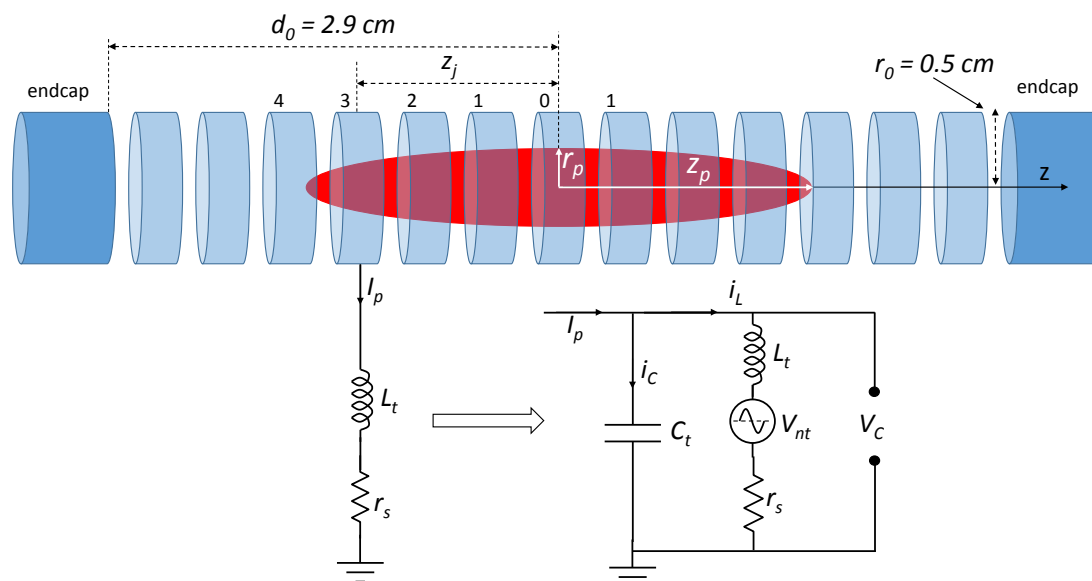
Figure 2. The AEḡIS open-ended cylindrical Penning trap and a tuned circuit connected to one electrode. The applied voltages and the plasma shape are symmetric with respect to the electrode labeled with index 0. The plasma occupies a consistent fraction of the trap length (the radial size is not to scale). The equivalent resonant circuit is also shown. C_t is dominated by the electrode capacitance.

a colder environment (100 mK in the final AEḡIS design). About 10^5 antiprotons (out of the $\simeq 3 \, 10^7$ delivered by the Antiproton Decelerator at CERN) are routinely caught in flight by fast switching the voltage of trap electrodes to 9 kV in the 5 T region. The antiprotons are then cooled by collisions with a plasma of more than 10^8 electrons pre-loaded in the same trap [8]. Electrons radiate their energy very efficiently in the high magnetic field and within few tens of seconds both of the species remain trapped within a potential well of few tens of Volts and in a few centimeters of length. Electrons and antiprotons are then adiabatically transferred toward the 1 T region of the trap system into the so-called antihydrogen production trap, where the antiprotons have to be cooled to a sub-Kelvin temperature before the antihydrogen production will take place. The energy of the antiprotons and electrons in the antihydrogen production trap is expected to be of the order of few K as was demonstrated for example in [9].

Reaching a sub-Kelvin antiproton temperature is an experimental challenge that in AEḡIS will be pursued by combining several techniques. One of them will investigate the use of a resistive cooling and detection circuit tuned to the axial resonance frequency of the electrons trapped in the antihydrogen production trap. The tuned circuit cools the axial motion of the electrons as was discussed in section 2.2 while their radial energy is dissipated by the cyclotron radiation and can reach a temperature quantum limit of 0.7 K (in a 1 Tesla magnetic field). Antiprotons will cool via Coulomb collisions with resistively cooled electrons.[1] The tuned circuit thus plays a crucial role as a cooling circuit as well as a diagnostic tool.

---

[1]The resistive cooling rate of many particles in a trap is not well documented and in addition the energy exchange between multiple trapped species at very low temperatures is also not well known. A discussion about the rate of energy exchange between the different degrees of freedom in a magnetized plasma of ions and electrons can be found in [10].

The experimental conditions of AEgIS differ from the ones where the tuned circuits are usually employed. The space-charge of many trapped particles is not negligible and the electron cloud forms a non-neutral plasma, which is sizable. Especially the axial dimension of plasma can occupy a large fraction of the trap length. This implies that the signal induced by the particle motion cannot be described by simply introducing a trap dependent geometrical constant α_0 like in section 2.1 and the plasma size and shape has to be correctly taken into account.

The antihydrogen production trap (see figure 2) consists of 13 electrodes with radius $r_0 = 5$ mm and equal length $L_{el} = 0.9 \ r_0$ with two longer end-caps. With a proper choice of the voltages applied to the electrodes one obtains a harmonic electric potential that approximates the standard hyperbolic Penning trap in a long region.

The following discussion is valid also for other cylindrical Penning trap geometries (for example [13]) as long as they maintain a harmonic potential profile in the volume, which could be occupied by the particle cloud. A single trapped particle axially oscillates with the characteristic frequency ω_z related to voltage difference V_0 between the central electrode and the end-cap:

$$\omega_z = \sqrt{\frac{qb_0V_0}{md_0^2}}, \tag{2.5}$$

where m is the particle mass and d_0 is the distance between the trap centre and the end-cap electrode (see figure 2). b_0 is a geometrical factor whose value is of the order of 1.

The number of electrons (ranging from 10^6 to several 10^8), their density (from less than 10^6 to several 10^8 cm^{-3}) and their temperature (from thousands of Kelvin to 100 mK) make the system behave as a cold non-neutral plasma [5]. The plasma shape and size at thermal equilibrium are thus determined by the trapping fields, the plasma central density, mean radius and temperature. In general the plasma density drops down within a distance of few Debye lengths. We assume that the radial size of the plasma is small compared to the trap radius and thus we neglect the effect of the electric field generated by the image charges in the determination of the plasma equilibrium shape.

When the plasma size is much larger than its Debye length the plasma shape is well approximated using the so-called zero temperature limit in which it forms an ellipsoid of uniform density with sharp edges and a radius r_p and an axial half length z_p.

A cold non-neutral plasma oscillates with predictable mode frequencies [11]. We will see that when a cold plasma is trapped in a Penning-like trap the tuned circuit detects the lowest order axial mode. This is a rigid oscillation of the whole plasma along the z-axis with the single particle axial motion frequency of eq. (2.5), without changes of its shape.

2.4 Tuned circuit detection of cold non-neutral plasma in Penning trap

In this section we provide a description of the signal induced by a harmonically confined cold non-neutral plasma on an electrode of an open-ended cylindrical Penning trap (see figure 2). We start with relations (2.2) and (2.1). The charge $Q_j(\vec{r}_k)$ induced on the electrode j when a generic particle of the plasma (labeled with the index k) is in the position $\vec{r}_k$ is obtained by solving an electrostatic

problem. The weighting field W_j of electrode j satisfies

$$\begin{cases} \nabla^2 W_j = 0 & \text{inside the trap} \\ W_j = 1 & \text{on the electrode j} \\ W_j = 0 & \text{on the other electrodes} \end{cases} \tag{2.6}$$

and (due to the symmetry of the electrodes) it depends only on the radial ρ_k and axial z_k cylindrical coordinates. While neglecting the radial velocity components we obtain the following simplified relation for the current $i_{jk}(t)$ induced by the axial motion

$$i_{jk}(t) \simeq q\frac{dz_k}{dt}\frac{\partial W_j(\rho_k, z_k)}{\partial z_k} \tag{2.7}$$

It is useful to define a new dimensionless geometrical factor α_j through the relation

$$\frac{\partial W_j(\rho_k, z_k)}{\partial z_k} = \frac{\alpha_j(\rho_k, z_k)}{2d_0} \tag{2.8}$$

In this definition d_0 can be replaced by any other characteristic trap length; the above definition was chosen to be similar to the hyperbolic Penning trap nomenclature. Note that $\alpha_j(\rho_k, z_k)$ depends on the position of the particle k while the geometrical factor α_0 introduced in eq. (2.3) becomes a constant $\alpha_0 = \alpha_j(0,0)$. The current induced on the tuned circuit by the axial motion of the particle k thus becomes

$$i_{jk}(t) = q\frac{dz_k}{dt}\frac{\alpha_j(\rho_k, z_k)}{2d_0} \tag{2.9}$$

The current induced by the plasma is the sum of the currents induced by each particle.

The ensemble of trapped particles and the tuned circuit are a coupled system that can be described by a set of differential equations linking the particle motion to the signal induced in the LC circuit. Referring to the circuit model shown in figure 2, we first consider the equation of motion of a generic particle k:

$$m\frac{d^2 z_k}{dt^2} = -m\omega_z^2 z_k - qV_C\frac{\alpha_j(\rho_k, z_k)}{2d_0} + \sum_{l \neq k} F_{lk}, \tag{2.10}$$

where in addition to the trap harmonic force $-m\omega_z^2 z_k$ we include also the force caused by the electric field generated by the tuned circuit. This electric field, which gives rise to the third term of eq. (2.10), is expressed using the weighting function of eq. (2.8) multiplied by the potential V_C created across the tuned circuit. The last term of the above equation is the sum of the Coulomb forces F_{lk} between all the particles.

The system of equations describing the circuit and the particle motion can be written as

$$\begin{cases} \dfrac{d^2 z_k}{dt^2} = -\omega_z^2 z_k - q\dfrac{V_C}{2md_0}\alpha(\vec{r}_k) + \sum_{lk} \dfrac{F_{lk}}{m} & k=1\ldots\text{N} \\[2ex] \dfrac{q}{2d_0}\sum_k \alpha_j(\rho_k, z_k)\dfrac{dz_k}{dt} = i_C + i_L \\[2ex] V_C = \displaystyle\int \dfrac{i_C(t)}{C_t}dt \\[2ex] -L_t\dfrac{di_L}{dt} - r_s i_L + \dfrac{1}{C_t}\displaystyle\int i_C(t)dt = V_{nt}(t) \end{cases} \tag{2.11}$$

where $V_{nt}(t)$ is the voltage noise associated to the resistor r_s. $V_{nt}(t)$ is a random function with mean value equal to zero and with non-null mean quadratic value $\bar{v}_{nt}^2$ already introduced in section 2.1.

The above system, with the additional inclusion of the equations for the radial motion, in principle describes the resistive cooling of the ensemble of N particles and the exchange of energy between them. The solution of the whole cooling problem of many particles and the evaluation of the cooling time is beyond the goal of this work. Some results obtained using numerical simulations are in [14]. Here we concentrate on the signal detected on the tuned circuit at equilibrium when the cooling of the particles has been achieved. For this reason we sum the motion equation over all N particles and we introduce the center of mass (CM) of the plasma with a coordinate $z_B = \sum_k z_k/N$. The terms due to the inter-particle Coulomb forces are eliminated and the equations are then greatly simplified to a form which is suitable for the study of the plasma collective axial motion at thermal equilibrium.

$$\frac{d^2 z_B}{dt^2} = -\omega_z^2 z_B - q\frac{V_C}{2md_0}\frac{1}{N}\sum_k \alpha_j(\rho, z) \tag{2.12}$$

Similarly to what is presented in [7] we introduce in the equation of the CM mass motion an additional term $-m\gamma\frac{dz_B}{dt}$ that describes the line-width of the CM motion and takes into account the coupling between the CM energy and the energy of the single particles. The introduction of the intrinsic line-width of the centre of mass motion is also a way to describe the realistic situation in which the frequencies of all the particles are not identical and show a distribution of values with a spread related to γ [15] (such frequency spread could be for example caused by the trap anharmonicities as a function of the radial position). The CM motion is then described by

$$\frac{d^2 z_B}{dt^2} = -\omega_z^2 z_B - \gamma\frac{dz_B}{dt} - q\frac{V_C}{2md_0}\frac{1}{N}\sum_k \alpha_j(\rho, z) \tag{2.13}$$

The total current induced by the plasma I_p is written as a sum of the currents induced by each particle:

$$I_p = i_C + i_L = \frac{q}{2d_0}\sum_k \alpha_j(\rho_k, z_k)\frac{dz_k}{dt} \tag{2.14}$$

Since the tuned circuit is highly selective in frequency, all the Fourier components of $z_k(t)$ with frequencies that largely differ from the resonance frequency are not relevant. The above consideration permits us to neglect the details of the motion of the single particles and to consider only the collective plasma motion with the axial frequency ω_z of eq. (2.5). The amplitude of this oscillation is related to the plasma temperature and it is small compared to the plasma dimensions. We calculate the current induced by this collective plasma movement by integrating the contributions of all the portions dN of particles of the plasma. If $f(\rho, z)$ is the distribution function of the number of particles in the plasma then

$$dN = 2\pi N \rho f(\rho, z) d\rho dz \tag{2.15}$$

where $\iint 2\pi \rho f(\rho, z) d\rho dz = 1$. The current induced by the axial oscillation of dN particles is

$$dI_p = q dN\frac{dz_B}{dt}\frac{\alpha_j}{2d_0} d\rho dz \tag{2.16}$$

and thus the overall current I_p induced by the plasma axial centre of mass mode is:

$$I_p = qN\frac{dz_B}{dt}\iint 2\pi \rho f(\rho, z)\frac{\alpha_j(\rho, z)}{2d_0} d\rho dz = qN\frac{dz_B}{dt}\frac{\alpha_{jp}}{2d_0} \tag{2.17}$$
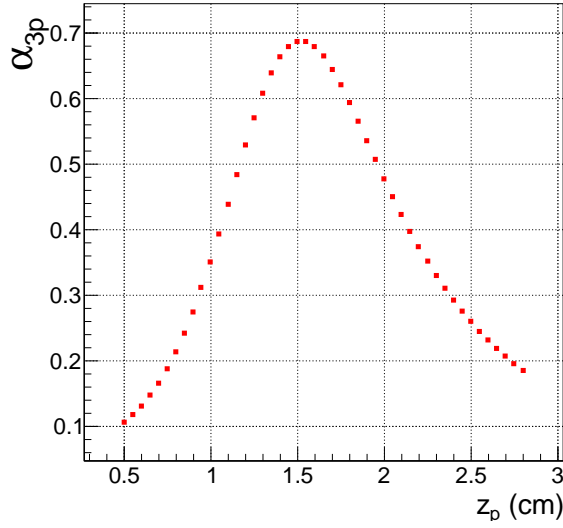
Figure 3. Values of α_{jp} as a function of z_p calculated for the AEḡIS trap when the tuned circuit is connected to the electrode number 3 assuming a ellipsoidal plasma in thermal equilibrium at zero temperature with constant density and radius $r_p = 2$ mm. The maximum current is obtained when the plasma length matches the distance of the pickup electrode from the trap centre.

where we have introduced a new geometrical factor α_{jp}

$$\alpha_{jp} \equiv 2\pi \iint \rho f(\rho, z)\alpha_j(\rho, z)d\rho dz, \tag{2.18}$$

which is not only dependent on the electrode dimension and position, but also depends on the plasma shape since we are integrating over the plasma volume. Figure 3 plots an example of α_{jp} as a function of the plasma half length. Relation (2.18) allows us to write I_p in a similar way to that of the current induced by few particles confined near the trap centre of eq. (2.3). The time dependence of α_{jp} originating from the movement of the particles within the plasma is not modeled. The validity of our approximation increases as long as the plasma temperature decreases. In general the effect of the particle motion can be phenomenologically included as a contribution to the damping term γ. Within our model the system of equations describing the coupling between the CM particle motion and the signal induced in the tuned circuit is

$$\begin{cases} \dfrac{dz_B^2}{dt^2} = -\omega_z^2 z_B - \gamma\dfrac{dz_B}{dt} - q\dfrac{V_C}{2md_0}\alpha_{jp} \\[2mm] i_C + i_L = \dfrac{qN}{2d_0}\dfrac{dz_B}{dt}\alpha_{jp} \\[2mm] V_C = \displaystyle\int \dfrac{i_C(t)}{C_t}dt \\[2mm] \dfrac{V_{nt}(t)}{L_t} = -\dfrac{di_L}{dt} - \Gamma_s i_L + \omega_0^2 \displaystyle\int i_C(t)dt \end{cases} \tag{2.19}$$

where we have also defined $\Gamma_s = r_s/L_t$.

The solution of the previous set of equations is the sum of the general solution of the homogeneous system plus a particular solution of the complete system. The latter describes the signals at equilibrium. We concentrate on this solution since all the approximations introduced before allow the description only at equilibrium. Writing $V_{nt}(t) = \int v_{nt} e^{i\omega t} d\omega$ and searching for solutions of the form $V_C(t) = \int V_{C0}(\omega) e^{i\omega t} d\omega$ we obtain

$$V_{C0}(\omega) = \frac{v_{nt}\,\omega_0^2\,(\Delta\omega_z^2 + i\omega\gamma)}{\Delta\omega_0^2\,\Delta\omega_z^2 - \omega^2\,\Gamma_s(\gamma + N\,\gamma_z) + i\omega\left[\Gamma_s\Delta\omega_z^2 + \gamma\Delta\omega_0^2 + N\,\gamma_z\Gamma_s^2\right]}, \qquad (2.20)$$

where $\Delta\omega_z^2 \equiv \omega_z^2 - \omega^2$ and $\Delta\omega_0^2 \equiv \omega_0^2 - \omega^2$.

The quantity $N\gamma_z = \frac{q^2 N \alpha_{jp}^2 Q_s^2 r_s}{4 d_0^2 m}$ is the CM mode resistive cooling rate. The power spectrum $V_{C0}^2(\omega) d\omega$ is the quantity which can be measured (after a suitable amplification). It is also useful to define Q_p (through $\gamma = \omega_z/Q_p$) which describes the width of the plasma resonance line.

Relation (2.20) reduces to that obtained for N particles trapped near the centre of the hyperbolic Penning trap if α_{jp} is replaced by α_0. An important feature of the above calculation is that for a sizable plasma its shape and the particle number are both included in the expression (2.20). Figure 4 shows an example of an ideal power spectrum obtained using the equation (2.20). The "dip" at the resonance frequency is expected also for the extended plasma, but the peak separation is related also to the plasma shape and not only to N. Nevertheless the tuned circuit still provides a useful information since the presence of the dip is a signature of a thermal equilibrium between the plasma and of the LC circuit. During the cooling process, when the particle temperature will be much higher than that of the tuned circuit, we expect to observe a peak[2] instead of a "dip" since the plasma would behave as a signal generator. We could thus estimate the rate of resistive cooling of the plasma from the time it takes to reach a stable "dip" configuration in the signal spectrum.

Arguments reported in [4] demonstrate that the particle temperature at equilibrium is determined by the temperature of the resistor and of the amplifier chain. Such arguments are valid also for a plasma provided that the energy exchange between the particles is efficient enough so that the continuous resistive cooling of the centre of mass mode results in cooling of all the particles.

3 Cryogenic amplifier performance

When an amplifier is connected to the tuned circuit the ultimate particle temperature is determined both by the Johnson noise of the resistor r_s and by the noise introduced by the amplifier itself. A key issue in the tuned circuit particle detection method is then the realization of a low-noise amplifier, which ensures a high signal-to-noise ratio and does not warm up significantly the trapped particles. Since it is useful to keep the capacitance of the circuit low and since the electronic noise is strongly dependent on the temperature, it is favorable to mount the low-noise amplifier as close as possible to the detection electrode in the cryogenic setup. This leads to another important requirement: a low power consumption (dissipation) of the amplifier. We have chosen high electron mobility transistors (HEMT) as promising devices for our amplifier design due to their excellent low noise and high gain characteristics; they are also known to work in a cryogenic environment. The data sheets report the performances at room temperature and at frequencies much higher than those

---

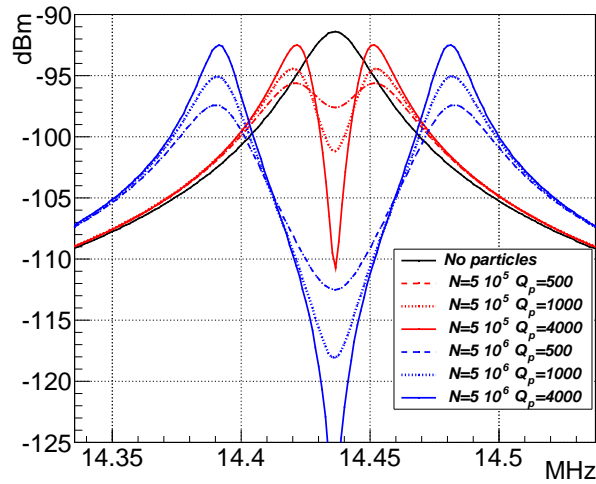[2]Similar to the single particle regime.

Figure 4. Calculated (black plot) noise power spectrum across the tuned circuit without particles including only the noise of r_s. The central frequency, the vertical axis normalization and the $Q_s = 545$ are the ones of the measurements described latter in this text. The red and blue curves show a calculation of the signals at equilibrium with this tuned circuit connected to the electrode 3 of figure 2 with trapped plasmas with $\alpha_{3p} = 0.5$. The number of particles and Q_p are reported in the plot.

of our interest. Direct measurements in the 10-20 MHz range were necessary. Our low noise cryogenic amplifier is made using a single pHEMT ATF34143 (AVAGO) transistor. Figure 5 shows the full schematic of the amplification chain including the tuned circuit, the cryogenic amplifier (referred to as cryoamplifier) with the above mentioned HEMT and a second amplifier operated at room temperature (referred to as RT amplifier). The design of the present amplifier is very simple and it uses a single HEMT (HEMT1) in a common source configuration. The focus of this work was to measure the performances of a HEMT-based amplifier coupled to the tuned circuit under our experimental constraints and extract its contribution to the noise. Alternative configurations, like a cascode scheme using two HEMTs may be considered. In the cascode scheme a common gate HEMT (called HEMT2) is cascaded to a common source HEMT (HEMT1). The advantage of this configuration with respect to our scheme is the potential reduction of the back-action toward the gate of HEMT1 due to the drain to gate capacitance. However in our experimental conditions this advantage is extremely limited: the ratio between the voltage developed at the drain of HEMT1 in the cascode and the common source scheme is Z_s/R_0. Z_s is the cascode input resistance which is related to the transconductance g_m through $Z_s \simeq 1/g_m$ and $R_0 = 50\Omega$ is the room temperature amplifier input resistance. A cascode is truly convenient when $Z_s/R_0 \ll 1$, but this condition is not easy to achieve within our experimental constraints.

The cryoamplifier is assembled on a low-loss teflon board housed in a copper box, on which a cylindrical copper shield of 17 mm inner diameter and 30 mm inner length is used to house the inductor of the tuned circuit. We have built a $L_t = 2.09 \pm 0.04 \mu H$ helical inductor 25 mm long formed by 23 turns of 0.7 mm diameter copper wire (enamelled) wound on a 10 mm diameter MACOR support of 1.5 mm wall thickness. In the AE\={g}IS apparatus the same inductor is connected
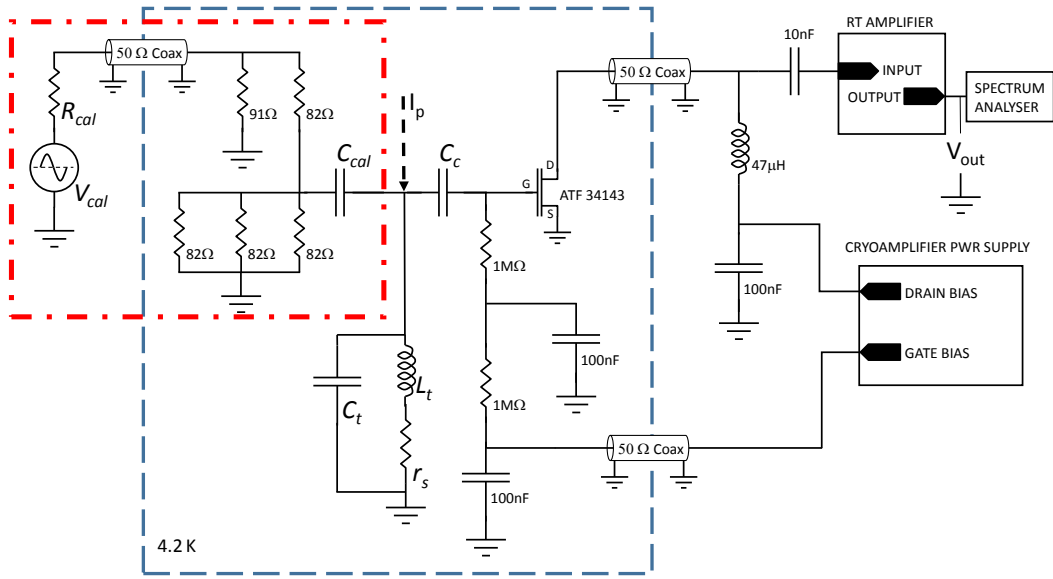
Figure 5. The full measurement circuit with the cryoamplifier (HEMT) at 4.2 K (inside the blue dotted line) and the room temperature amplifier. The elements inside the red dotted-dashed box represent the signal generator and the attenuator coupled to the tuned circuit with C_{cal} and used in the noise measurement setup to calibrate the gain of the circuit. These elements are not present when the tuned circuit and the amplifier are connected to the trap: in that case the input signal is the current I_p induced by the trapped particles (shown with a dotted line).

to a trap electrode and along with its capacitance it forms the tuned circuit.[3] The correct frequency is adjusted by adding a short piece of rigid radio-frequency cable that acts as a small high quality capacitor. During the cryoamplifier noise and performance measurements, where the trap was not present, we emulated the trap capacitance with a high Q capacitor (C_t in figure 5) in order to reach the nominal resonance frequency. In addition the components designed within the blue dotted box of figure 5 were immersed inside a liquid helium dewar, whereas in the AEḡIS apparatus they are mounted in a vacuum chamber kept at 4.2 K or below. The cryoamplifier is coupled via a coupling capacitor $C_c = 150$ pF to the tuned circuit and it is thus in the same configuration as during normal operation in AEḡIS . In this way we can measure the important parameters like the noise, gain and power consumption in the same working condition achievable when the cryoamplifier and the tuned circuit are connected to the trap.

The response function of the full circuit of figure 5 has been obtained using a PSPICE model. Several parameters have been fixed since they can be directly measured. The inductor L_t and the capacitor C_t are the elements of the unloaded resonant circuit: its resonance frequency is $f_0 = \omega_0/(2\pi) = 14.46$ MHz and its (unloaded) quality factor is $Q_{\mathrm{unl}} = 655$. The series resistance is $r_s = 0.29\,\Omega$ (calculated using $Q_{\mathrm{unl}} = \dfrac{\omega_0 L_t}{r_s}$) and the equivalent parallel resistance at resonance is R_d =124 $k\Omega$. The sinusoidal generator V_{cal} with its internal resistance $R_{\mathrm{cal}} = 50\,\Omega$ was used to calibrate the gain of the full amplifier chain by exciting the tuned circuit with a signal of known amplitude

---

[3]Since the current AEḡIS temperature may not reach 4.2 K we have chosen a simple copper wire. An improved higher quality superconducting coil has been tested and it is foreseen.
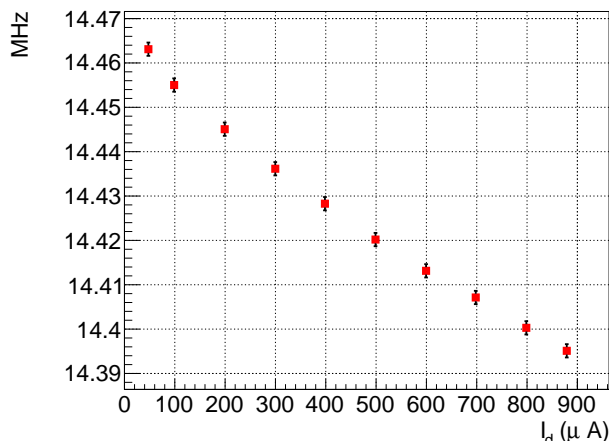
Figure 6. The circuit resonance frequency (MHz) as a function of the HEMT drain current I_d.

at the resonance frequency f_0. The generator input power of -110 dBm is sufficient to produce an output signal more than 20 dB above the noise level. The capacitor $C_{cal} = 0.90 \pm 0.05$ pF is used to couple the signal generator to the tuned circuit.[4] In order to reduce the contribution of the room temperature Johnson noise of R_{cal} we have inserted a 12 dB attenuator at helium temperature on the generator signal line. Two series resistors $R_{bias} = 1$ MΩ are used to supply the bias to the gate of the HEMT, which is modeled as a device with an ideal transconductance g_m, a capacitance C_{gd} between gate and drain and a capacitance C_{gs} between the gate and the source.

The load of the tuned circuit and the decrease of the quality factor due to its capacitive coupling to the HEMT is tolerable with Q^{load} ranging from 602 to 545 depending on the working conditions. The dynamic resistance is reduced accordingly to $R_d^{load} = 119 - 108$ $k\Omega$. The loading (and also the back action and the heating effects) of the amplifier could be reduced by decoupling it inductively or capacitively from the tuned circuit at the cost of reducing the signal-to-noise ratio. The present configuration offers the maximal sensitivity to the measurement of the HEMT gate radio-frequency impedance.

The PSPICE simulation models all the components of the circuit, including the 50 Ω cable connecting the cryogenic amplifier to the RT amplifier. The 3.6 m long cable influences the response function of the circuit due to the input return loss of the RT amplifier (the output impedance of the cryoamplifier is 400 Ω while the input impedance of the RT amplifier is $R_0 = 50$ Ω).

3.1 Gain and power consumption

We obtained a stable HEMT working point by first setting the drain-source voltage V_d and then adjusting the gate voltage V_g to maintain constant drain-source current I_d. The value of the transconductance g_m, which determines the gain of the HEMT, is thus fixed. We observed (see figure 6) a decrease of the resonance frequency as I_d increases. This could be due to an effective increase of the capacitance in parallel to the tuned circuit as expected by the Miller effect [16]. The transconductance and the gate-drain capacitance $C_{gd} = 0.28$ pF have been extracted from the simulation in a self-consistent manner by requiring the simulation to reproduce the measured output power

---

[4]The value of this capacitor at 4.2 K has been precisely measured since it influences the determination of the gain.
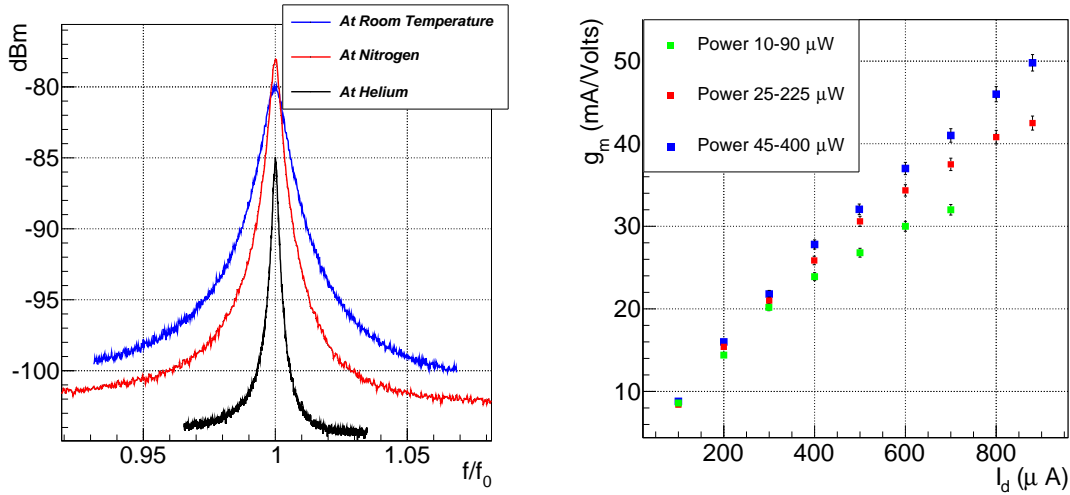
Figure 7. *Left*: output power spectrum at room temperature, 77 K and at 4.2 K without any external drive or trapped particle signal. All measurements were performed with $V_g = 300$ mV, and $I_d = 300$ mA. The resolution bandwidth is 30 kHz. The increase of the quality factor from 77 K to 4.2 K is mainly due to the decrease of the resistivity of the copper wire used for building the coil as a function of the temperature. *Right*: g_m measured at 4.2 K as a function of I_d for 3 different values of V_d and thus of dissipated power. V_g varies in the range from -250 to -320 mV.

at resonance when using the signal generator and at the same time to reproduce the shift of the resonance frequency as a function of I_d. The gate-source capacitance $C_{gs} = 0.8$ pF is taken from the ATF34143 data-sheet. We reproduce the resonance shift within approximately 2 kHz.

Figure 7 (left) shows the power spectrum around the resonance frequency at the output of the whole amplifier chain in the absence of any external signal drive. In the three shown cases the drain voltage V_d is adjusted to obtain the same drain current I_d. In figure 7 (left) the drive signal of the resonant circuit is represented by the various noise sources of the circuit itself. The differences among the three curves shown in figure 7 (left) are the cumulative effect of: the change of the HEMT gain while the temperature decreases; the reduction of the noise (drive level); the increase of the Q-factor of the copper tuned circuit at low temperature.

Figure 7 (right) shows the transconductance g_m of the HEMT at 4.2 K as a function of the drain current. The accuracy of the gain measurement along with the simulation error are 0.15 dB. The three curves correspond to three different drain voltages ($V_d = 100, 250, 450$ mV): both the drain voltage and the drain current are significantly lower than that needed at room temperature to obtain a similar gain. This increase of gain of the HEMT at low temperature allows keeping low power dissipation and makes this device a promising candidate to be used inside a dilution refrigerator. The power consumption ranges from few tens to few hundreds of μW. At maximum drain current and drain voltage explored during the cryogenic measurements the dissipated power was 400 μW and the transconductance reaches a value of 50 mA V^{-1}. The cryoamplifier power gain at resonance is $G_{\text{pow}} = \frac{V_{\text{cryo}}^2/R_0}{I_p^2 R_d^{\text{load}}}$ where V_{cryo} is the cryoamplifier output voltage. Being $V_{\text{cryo}} \simeq g_m I_p R_0$ then $G_{\text{pow}} = g_m^2 R_0 R_d^{\text{load}}$ that corresponds to about 95 dB if $g_m = 50$ mA V^{-1}.
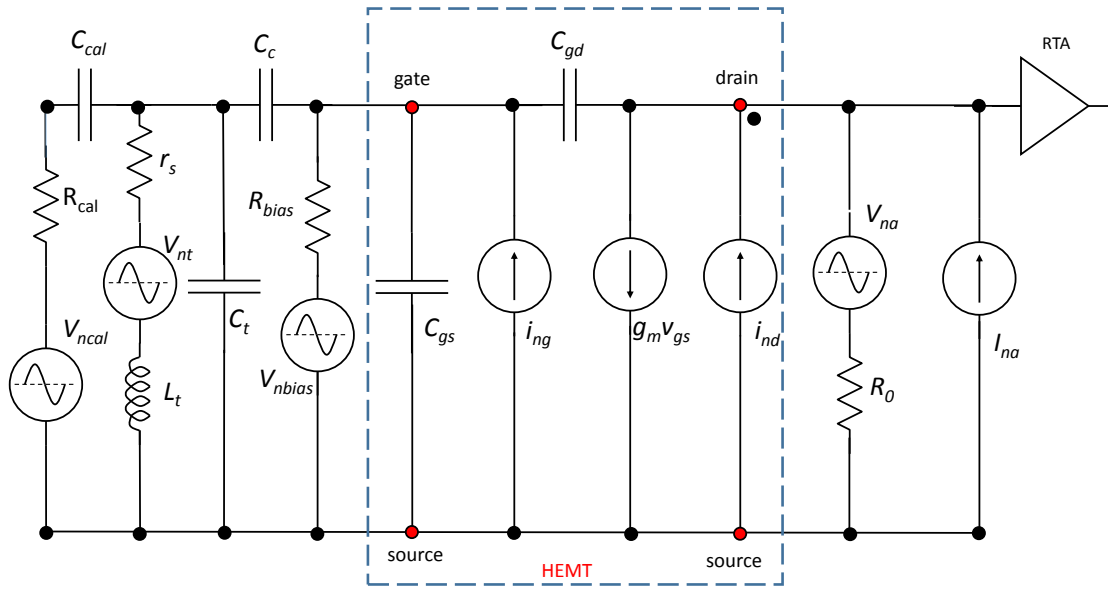
Figure 8. Noise scheme showing all the contributions. The elements in the dashed box represent the HEMT.

3.2 Noise analysis model

Noise in HEMT devices, as in other semiconductor devices, originate from several physical mechanisms. The main noise sources are the thermal noise, diffusion noise, shot noise, gate leakage and 1/f noise. Usually HEMT are operated at microwave frequencies and the thermal noise due to the diffusion of the carriers in the channel is the dominant contribution [21]. In the very low frequency range (well below 1 MHz) gate leakage noise is measured to be significant [20]. Since our frequency of operation is in the intermediate range it is hard to predict a priori the dominant contribution. Noise models based on small signal parameters are widely used to describe the measured results. We have used the scheme of figure 8 where, in addition to the contribution of the HEMT, we have included the noise of all the other elements of our circuit. The dominant contribution to the thermal noise of the HEMT is identified in the literature as the drain current noise I_{nd} with mean spectral power $\overline{i_{nd}^2}$

$$\overline{i_{nd}^2} = 4KT_d g_{ds} \Delta f \tag{3.1}$$

where g_{ds} is a conductance whose value is model dependent. For reference, in [19] and [17] g_{ds} is proportional to the the zero-bias drain conductance g_{d0} defined through the relation $g_{ds} = \gamma_g g_{d0}$, where $2/3 < \gamma_g < 1$ and T_d is the temperature of the device. In the description of [18] g_{ds} is the intrinsic drain conductance as resulting from the small signal model of the HEMT and T_d is an effective temperature that may be higher than the physical one. In the following discussion we will indicate by T_a the ambient temperature ($T_a = 300\,\mathrm{K}$) and by T_0 the liquid helium temperature ($T_0 = 4.2\,\mathrm{K}$).

An additional thermal noise source discussed in the literature is the induced gate current due to the capacitive coupling between the gate and drain. Following [17] we model this contribution as a white voltage noise that (due to the presence of C_{gs}) produces a current noise whose spectral

power rises with the square of the frequency. The resulting induced current gate noise I_{ng} with a mean spectral power $\overline{i_{ng}^2}$ is usually written as

$$\overline{i_{ng}^2} = 4KT_g\delta\frac{\omega^2 C_{gs}^2}{g_{gs}}\Delta f \tag{3.2}$$

In our case the value of the spectral power of the gate noise current is modified, because we cannot neglect the high value of the impedance of the tuned circuit, which is in series with C_{gs} (see figure 8). The simulation of the circuit accounts for the above mentioned effect; under our typical conditions $\overline{i_{ng}^2}$ is reduced by a factor of about 0.8 with respect to the value obtained from (3.2).

In the model of [19] $T_d = T_g$, $g_{gs} \simeq 5g_{d0}$ and the gate noise is partially correlated with the drain one. In the approach of [18] g_{gs} results from the intrinsic small signal model of the device and T_g is a free parameter. T_g is often similar to T_0 while T_d can be some order of magnitude higher; g_{ds} and g_{gs} lie typically in the range of few Ω^{-1}, but significant differences exist among different devices and operating conditions.

The HEMT noise contribution was extracted by fitting the noise-driven spectrum (measured when the system was immersed in liquid helium) with the sum of the spectra of the known noise sources. The individual noise spectra have been calculated with the PSPICE simulation using the circuit model in figures 5 and 8. Our results do not depend on any hypothesis about the specific values of T_d, T_g, g_{ds} and g_{gs}. Possible correlations among the various noise sources have been neglected. The amplitudes of the noise contributions not related to the HEMT are constrained or fixed by the results of dedicated measurements, while those relative to the HEMT are left as free fit parameters. This procedure is possible once the resonance frequency and the overall gain of the chain are reproduced by the simulation. We have included in total seven uncorrelated contributions to the noise spectrum:

- The Johnson noise of the resistor R_{cal} at the temperature T_a.

  The mean value of its spectral power is $\overline{v_{ncal}^2} = 4KT_a R_{cal}\Delta f$ and its effective temperature is reduced by the 12 dB attenuator immersed in liquid helium.

- The noise V_{nt} associated to the radio-frequency losses of the unloaded tuned circuit at temperature T_0 (discussed in section 2.1) with mean spectral power $\overline{v_{nt}^2} = 4KT_0 r_s\Delta f$.

- The Johnson noise of the gate bias resistor R_{bias} with mean spectral power $\overline{v_{nbias}^2} = 4KT_0 R_{bias}\Delta f$

- Two contributions originated from the room temperature amplifier: a current and a voltage noise. The mean values of the corresponding noise spectral powers have been measured and these contributions were modeled by introducing two resistors r_{na}^i and r_{na}^V, whose Johnson noise reproduces the measured mean noise power $\overline{v_{na}^2} = 4KT_a r_{na}^V\Delta f$ and $\overline{i_{na}^2} = 4KT_a r_{na}^i\Delta f$. The voltage noise is 0.78 nV Hz$^{-\frac{1}{2}}$ and the current noise is 18.5 fA Hz$^{-\frac{1}{2}}$ and the corresponding noise figure is about 4 dB.

3.3 Noise analysis results

We have measured the output power spectrum for several values of the the drain current I_d ranging from 100 to 900 μA working points. For each of these values, we have first reproduced with the
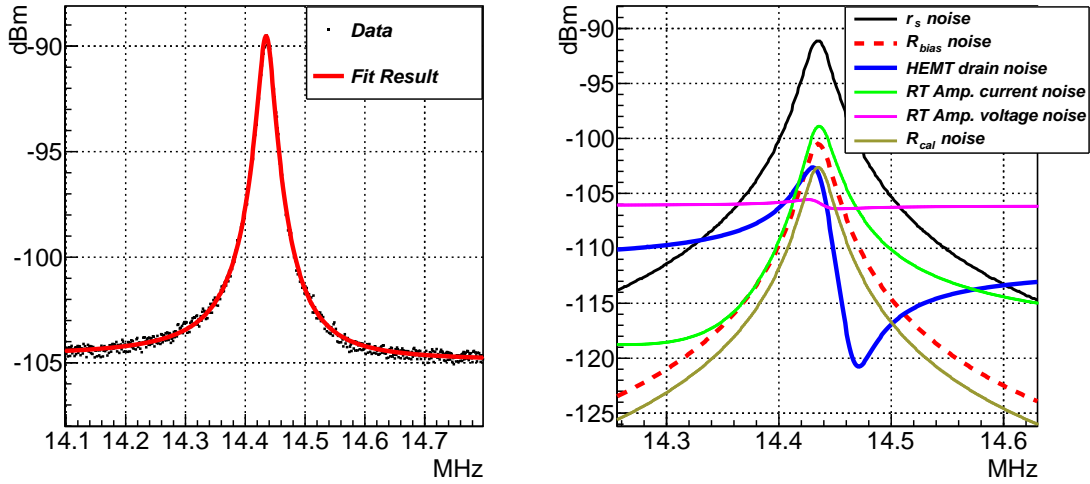
Figure 9. *Left*: the output power spectrum (dots) measured at 4.2 K ($I_d = 300 \mu$A, resolution bandwidth of 30 KHz, video bandwidth of 300 Hz) along with the fit results (red continuous curve). *Right*: the single components of the noise spectrum with the amplitudes resulting from the fit. The contribution of the HEMT gate noise is railed to zero. Note that the scales of the left and right plot are not the same.

simulation the measured cryoamplifier gain and thus fixed the transconductance g_m. Then we used the noise simulation to obtain the individual noise contributions to the total power spectrum as measured at the output circuit terminal.

These individual contributions once summed with proper weights reproduced the measured power spectrum. The best estimation of the cryoamplifier noise is obtained by minimising the χ^2 calculated with the measured output power spectrum and the sum of the contributions obtained with the simulation model as a function of the above mentioned amplitudes. During the minimization procedure the contributions of all the noise components that are not related to the cryoamplifier are allowed to vary only within the known experimental errors. Figure 9 (left) shows an example of the measured power spectrum with the fit superimposed. The black points are the experimental data. Figure 9 (right) displays the seven noise contributions with their respective amplitudes as a result of the fitting procedure. The fitted curves reproduce the data for all the considered working points (drain currents) indicating that the noise analysis model is able to describe the measured effects.

Note that the baseline noise of about -105.5 dBm is mainly determined by the voltage noise of the room temperature amplifier v_{na}^2. This amplifier was a good trade-off between its return loss and the noise figure. When the detection circuit will be installed in the trap cryostat it may be convenient to substitute this room temperature amplifier also with a cold one.

All the contributions besides i_{na}^2 and i_{nd}^2 have a very similar spectral shape: the asymmetry of i_{nd}^2 as a function of frequency is the key feature that allows us to clearly measure its contribution to the noise spectrum. Figure 10 (left) shows the values of the drain noise current as a function of I_d obtained using our noise analysis. We observe a value of $\overline{i_{nd}^2}$ weakly increasing with the bias drain current. The induced current gate noise $\overline{i_{ng}^2}$, on the other hand, significantly decreases as a function of I_d: non-zero contributions of $\sqrt{\overline{i_{ng}^2}} = 20 \pm 2$ fA Hz$^{-\frac{1}{2}}$ and 10 ± 2 fA Hz$^{-\frac{1}{2}}$ are measured only at the lowest drain current settings of $I_d = 100$ and 200μA respectively. For higher drain currents we
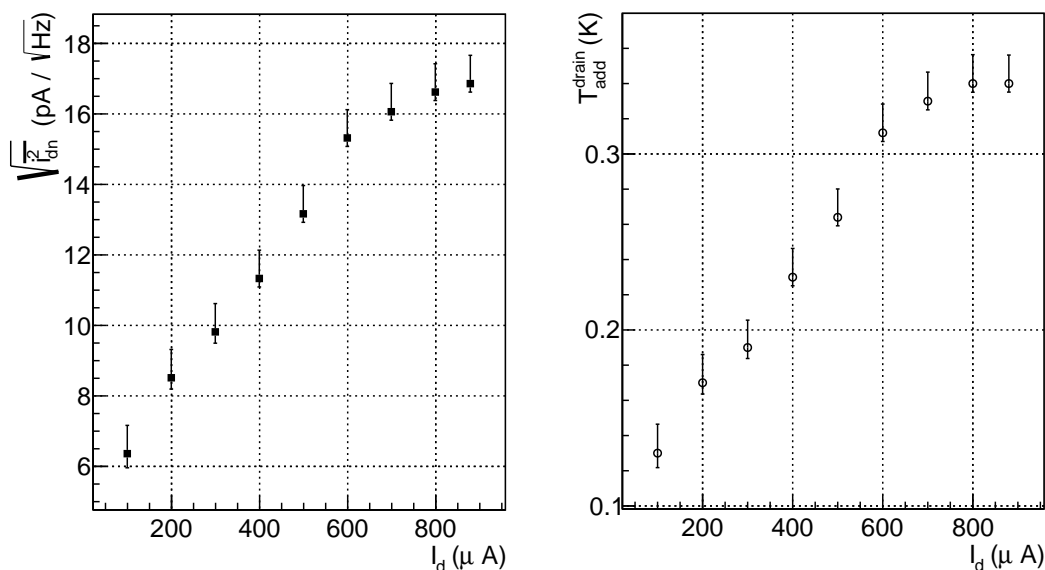
Figure 10. *Left*: mean value of the HEMT drain noise current per unit of bandwidth as a function of the bias current I_d. *Right*: equivalent added temperature of the tuned circuit due to the HEMT noise drain current as defined in the text.

can set the limit of this noise to $\sqrt{i_{ng}^2} < 2\,\mathrm{fA\,Hz}^{-\frac{1}{2}}$. The measured gate noise can be of non thermal origin: this is suggested by its strong dependence on the working conditions in fair agreement with [20].

We then analyzed the peak power of the signal across the tuned circuit. The noise of the HEMT can be described by introducing the temperatures $T_{\mathrm{add}}^{drain,gate}$ and identifying the peak power with the expression $4K(T_0 + T_{\mathrm{add}}^{drain,gate})R_d^{\mathrm{load}}\Delta f$, to be compared to the the value $4KT_0R_d^{\mathrm{load}}\Delta f$ that would be obtained if the HEMT was not present. Figure 10 (right) shows $T_{\mathrm{add}}^{\mathrm{drain}}$ as a function the HEMT drain current: note that the $T_{\mathrm{add}}^{\mathrm{drain}}$ is 0.35 K at maximum. For the gate noise contribution we get $T_{\mathrm{add}}^{\mathrm{gate}} < 0.02$ K for $I_d \geq 300\mu A$ and $T_{\mathrm{add}}^{\mathrm{gate}} = 0.63$ (0.31) for $I_d = 100$ (200) μA respectively.

The error bars in figure 10 originate from the spread of the distribution of the values obtained by repeating the noise analysis several times after having changed the input model parameters within their experimental errors. The uncertainties obtained fitting each single measurement (with fixed working conditions and parameters of the circuit) are smaller. Within the uncertainties of the measurement we did not observe a dependence of i_{nd} and i_{ng} on the drain-source voltage V_d.

The signals shown in figure 4 represent the spectra measured under the ideal conditions across the tuned circuit at equilibrium when the trapped plasma is driven only by the noise of the resistance r_s. In the case of a real tuned circuit connected to a trap the additional noise components that were discussed previously provide a further drive and they influence the shape of the output signal. Figure 11 compares the signal measured with the setup described in the previous pages with a calculation of the expected signal from $5 \cdot 10^6$ and $5 \cdot 10^7$ electrons at equilibrium and Q_p being the same as in figure 4. This time we have included all the expected additional noise sources present in the circuit. The lowest level of the dip that could be measured is determined, in our conditions, by the voltage noise of the room temperature amplifier (which is responsible for the baseline of
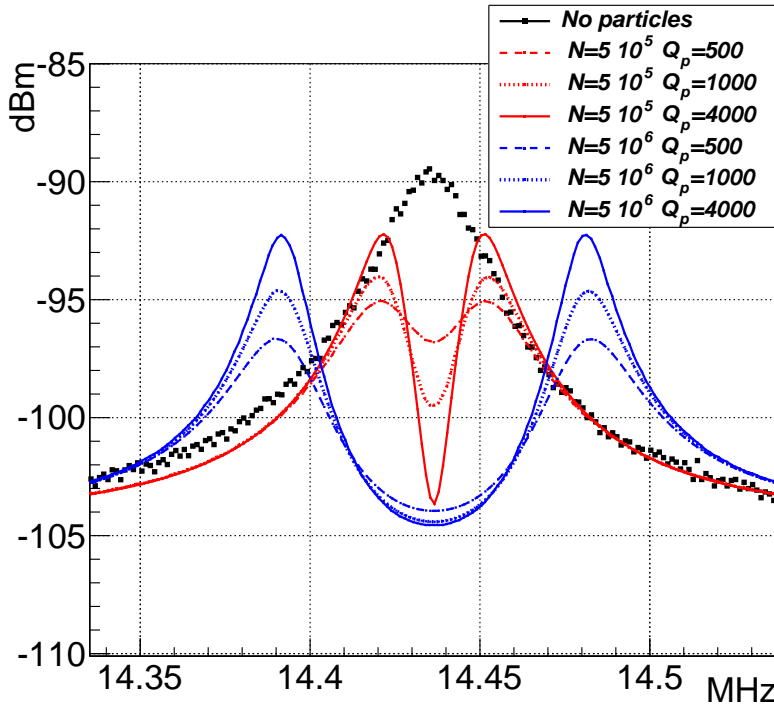
Figure 11. The black dotted points are the power spectrum measured without particles with $I_d = 300\mu A$, a resolution bandwidth of 30 KHz and a video bandwidth of 300 Hz. The red and blue curves show a calculation of the expected signal with trapped particles in thermal equilibrium with the tuned circuit (with the same conditions as in figure 4) taking into account all the noise sources. This figure should be compared with figure 4.

the spectrum) and we are not influenced in a sensitive way by the cryoamplifier noise. As was mentioned earlier the RT amplifier was not optimized during this work and could be replaced by a lower noise (even cold) device in the future.

4 Conclusions

Cooling to sub-Kelvin temperatures and detecting a non-neutral electron plasma is of primary importance in the AEḡIS experiment and in every experiment working with low energy anti-hydrogen. We have presented a consistent model allowing the prediction of the signal induced by a sizable cold plasma trapped in a cylindrical Penning trap and in equilibrium with a tuned circuit. The induced signal is influenced by the shape of the plasma, through the geometrical factor α_{jp}. However the main features of the tuned circuit remain unchanged with respect to its use with few particles.

We have built a cryogenic amplifier based on a single pHEMT ATF34143 (AVAGO) transistor coupled to a resonant circuit tuned to the frequency of the axial motion of an electron plasma (14.4 MHz) and we have tested it at the temperature of 4.2 K. We have obtained excellent performance at this frequency and temperature with low noise, high gain and low power consumption. The result make the tuned circuit coupled with this amplifier a promising device to be used also in a trap environment colder than 4.2 K.

Acknowledgments

References

[1] AEGIS collaboration, M. Doser et al., *Exploring the WEP with a pulsed cold beam of antihydrogen*, *Class. Quantum Grav.* **29** (2012) 184009.

[2] AEGIS collaboration, S. Aghion et al., *A moire deflectometer for antimatter*, *Nat. Commun.* **5** (2014) 4538.

[3] F.G. Dehmelt and F.L. Walls, *"Bolometric" technique for the rf spectroscopy of stored ions*, *Phys. Rev. Lett.* **21** (1968) 127.

[4] L.S. Brown and G. Gabrielse, *Geonium theory: physics of a single electron or ion in a Penning trap*, *Rev. Mod. Phys.* **86** (1986) 58.

[5] D.H.E. Dubin and T.M. O'Neil, *Trapped nonneutral plasmas, liquids, and crystals (the thermal equilibriumstates)*, *Rev. Mod. Phys.* **71** (1999) 87.

[6] Z. He, *Review of the Shockley-Ramo theorem and its application in semiconductor gamma-ray detectors*, *Nucl. Instrum. Meth.* **A 463** (2001) 250.

[7] D.J. Wineland and H.G. Dehmelt, *Principles of the stored ion calorimeter*, *J. Appl. Phys.* **46** (1975) 919.

[8] AEGIS collaboration, D. Krasnický et al., *AEgIS experiment commissioning at CERN*, *AIP Conf. Proc.* **1521** (2013) 144.

[9] G. Gabrielse et al., *Adiabatic cooling of antiprotons*, *Phys. Rev. Lett.* **106** (2011) 073002.

[10] H. Nersisyan, C. Toepffer and G. Zwicknage, *Interactions between charged particles in magnetic fields*, Springer, Germany (2007).

[11] D.H.E. Dubin, *Theory of electrostatic fluid modes in a cold spheroidal non-neutral plasma*, *Phys. Rev. Lett.* **66** (1991) 2076.

[12] X. Feng et al., *Tank circuit model applied to particles in a Penning trap*, *J. Appl. Phys.* **79** (1996) 8.

[13] ATHENA collaboration, M. Amoretti et al., *The ATHENA antihydrogen apparatus*, *Nucl. Instrum. Meth.* **A 518** (2004) 679.

[14] G. Maero, *Cooling of highly charged ions in a Penning trap for HITRAP*, *Ph.D. Thesis*, University of Heidelberg, Heidelberg, Germany (2008).

[15] N. Beverini et al., *Stochastic cooling in Penning traps*, *Phys. Rev.* **A 38** (1988) 107.

[16] J.M. Miller, *Dependence of the input impedance of a three-electrode vacuum tube upon the load in the plate circuit*, *Scientific Papers of the Bureau of Standards* **15** (1920) 367.

[17] D.K Shaeffer and T.H. Lee, *A 1.5 V, 1.5 GHz CMOS low noise amplifier*, *IEEE J. Solid-St. Circ.* **32** (1997) 1.

[18] M.W. Pospieszalski, *Modeling of noise Parameters of MESFET's,and MODEFET's and their frequency and Temperature dependance*, *IEEE Trans. Microw. Theor. Techn.* **37** (1989) 1340.

[19] A. Van Der Ziel, *Thermal noise in field effect transistors*, *Proc. IRE* **50** (1962) 1808.

[20] Y.X.Liang, Q. Dong, U. Gennser, A. Cavanna and Y. Jin, *Specific HEMTs for deep cryogenic high-impedance ultra low low-frequency noise read-out electronics*, *J. Phys. Conf. Series* **400** (2012) 052015.

[21] M.W. Pospieszalski, *Extremely low-noise amplification with cryogenic FETs and HFETs: 1970–2004*, *IEEE Microw. Mag.* **6** (2005) 62.